

Analytical explanation of phase transitions in the multifractal measure derived from a one-dimensional random field Ising model

Heiko Patzlaff, Thomas Nowotny and Ulrich Behn

Institut für Theoretische Physik, Universität Leipzig
Augustusplatz 10, 04109 Leipzig, Germany

May 19, 2019

Abstract

In certain one-dimensional stochastic iterated function systems a sharp drop in the D_q -spectrum of generalized fractal dimensions for negative q is observed at a critical value of the noise strength h . This transition is connected with the disappearance of deep cuts in the measure density and can be understood by an analysis of the contribution of periodic orbits to the measure. We discuss a special example derived from a one-dimensional Ising model in a bimodal random field.

PACS numbers: 05.45.Df, 05.50.+q, 75.10.Nr, 05.70.Fh

1 Introduction

We consider the one-dimensional random field Ising model [1]-[13]. Its Hamiltonian is given by

$$H = - \sum_{i=1}^{N-1} J s_i s_{i+1} + \sum_{i=1}^N h_i s_i, \quad (1)$$

where s_i denotes the classical spin at site i which takes values 1 or -1 and J is the exchange energy of adjacent spins. The local magnetic fields $\{h_i\}$ at the sites $i = 1, \dots, N$ are independent identically distributed random variables. We restrict ourselves to bimodal distributions with probability densities

$$\rho(h_i) = p_+ \delta(h_i - h_+) + p_- \delta(h_i - h_-). \quad (2)$$

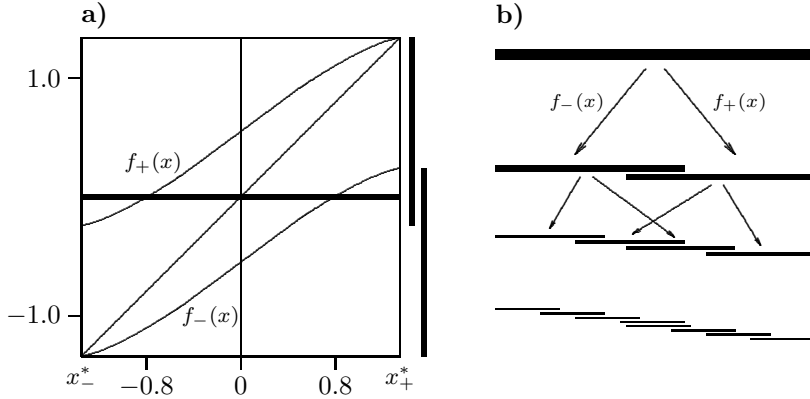


Figure 1: (a) Mapping in the case of overlapping bands $I_+ = f_+(I)$ and $I_- = f_-(I)$. In (b) the first few images of the interval I are shown. The increasing complexity of the band structure is obvious. ($h = 0.55$, $\beta = 1$, $J = 1$ in both figures.)

An iterative reformulation of the canonical partition function yields the partition function of a single spin in an effective external random field x_N given by an iterative map [2],

$$x_n = h_n + A(x_{n-1}), \quad x_0 = 0 \quad (3)$$

$$A(x) = \frac{1}{2\beta} \ln \left(\frac{\cosh \beta(x+J)}{\cosh \beta(x-J)} \right), \quad (4)$$

where β denotes the inverse temperature.

The mapping defines a stochastic trajectory which in turn yields an invariant probability measure $dP_\infty(x)$, the probability of the trajectory to visit the small interval dx centered around x . The iteration has an attractor which is a subset of the interval $I = [x_-^*, x_+^*]$, bounded by the fixed points x_\pm^* of the functions $f_\pm(x) = A(x) + h_\pm$.

The maps f_\pm are contractive and thus iterations of f_+ and f_- are also contractive. Therefore the first image of the interval I consist of two smaller ‘bands’ I_+ and I_- which may or may not overlap, depending on the value of the parameters h_+ and h_- . In the following we restrict ourselves to a symmetric distribution $p_+ = p_- = 0.5$, $h_+ = -h_- = h$ (cf. Figure 1). For the case of a non-symmetric distribution see [5].

We consider the integrated probability distributions (the measures) $P_n(x)$ of the interval $(-\infty, x)$ which we iteratively construct using the Frobenius-Perron

equation

$$\begin{aligned} P_n(x) &= \int dh \rho(h) P_{n-1}(A^{-1}(x-h)) \\ &= \sum_{\sigma=\pm} p_\sigma P_{n-1}(f_\sigma^{-1}(x)). \end{aligned} \quad (5)$$

The fixed point of (5) gives the natural invariant measure $P_\infty(x)$ for almost all initial measures $P_0(x)$. This invariant measure determines the effective random field x of our auxiliary one-spin system in the thermodynamic limit $N \rightarrow \infty$.

To investigate the structure of the measure we consider a finite iteration of order n of an arbitrary smooth initial measure P_0 and take the limit $n \rightarrow \infty$ at the end. The iteration is realized by the 2^n composite functions $f_{\{\sigma\}_n}$

$$f_{\{\sigma\}_n} = f_{\sigma_n} \circ f_{\sigma_{n-1}} \circ \dots \circ f_{\sigma_1}, \quad (6)$$

where $\{\sigma\}_n$ denotes the symbolic sequence of n plus and minus signs $\{\sigma\}_n = \sigma_n \sigma_{n-1} \dots \sigma_1$. We denote the fixed points of $f_{\{\sigma\}_n}$ as $x_{\{\sigma\}_n}^*$, $f_{\{\sigma\}_n}(x_{\{\sigma\}_n}^*) = x_{\{\sigma\}_n}^*$. Every function $f_{\{\sigma\}_n}$ maps the invariant interval onto a small band $I_{\{\sigma\}_n}$. Any such band carries a total weight of $(\frac{1}{2})^n$ and the measure P_n is a superposition of these bands. In taking the limit $n \rightarrow \infty$ all bands shrink to points because of the contractivity of the function $A(x)$. The limit points can be labelled by infinite sequences $\{\sigma\} := \{\sigma\}_\infty$. In the case of a periodic sequence $\{\sigma\} = (\{\sigma\}_n)_\infty$, the corresponding limit point is the fixed point $x_{\{\sigma\}_n}^*$ of $f_{\{\sigma\}_n}$. In the case of a non-periodic sequence we can approximate the corresponding limit point $x_{\{\sigma\}}^*$ by $f_{\{\sigma\}_n}(x)$ in which $\{\sigma\}_n$ is the ‘head’ of the n leftmost symbols of $\{\sigma\}$, and x an arbitrary initial point in I . We generalize the concept of fixed points in the case of non-periodic sequences $\{\sigma\}$ by defining $f_{\{\sigma\}}(x) := \lim_{n \rightarrow \infty} f_{\{\sigma\}_n}(x)$ where $\{\sigma\}_n$ is again the head of $\{\sigma\}$. Clearly $f_{\{\sigma\}}(x_{\{\sigma\}}^*) = x_{\{\sigma\}}^*$, i.e. $x_{\{\sigma\}}^*$ is the fixed point of $f_{\{\sigma\}}$. In the case of a periodic sequence this coincides with the definition of the fixed points considered before, $x_{(\{\sigma\}_n)_\infty}^* = x_{\{\sigma\}_n}^*$.

To make the approximation of the invariant measure P_∞ explicit we iteratively apply the Frobenius-Perron equation to an initial measure $P_0(x)$ [5]. In the first iteration $P_1(x)$ is a sum of two terms that involve $P_0(x)$. $P_2(x)$ then is a sum of four terms and finally we get an expression for $P_n(x)$ as a sum of 2^n terms, involving P_0 at the predecessors $y_{\{\sigma\}_n}$ of x ,

$$P_n(x) = \sum_{\{\sigma\}_n} P_{\{\sigma\}_n}(y_{\{\sigma\}_n}), \quad (7)$$

$$P_{\{\sigma\}_n}(y_{\{\sigma\}_n}) = \frac{1}{2^n} P_0(y_{\{\sigma\}_n}), \quad (8)$$

$$y_{\{\sigma\}_n} = f_{\{\sigma\}_n}^{-1}(x). \quad (9)$$

For fixed x this is a path integral in the space of the symbolic dynamics.

In general, most of the terms vanish and only a small fraction of overlapping bands contribute to the measure at a specific point. For certain values of the

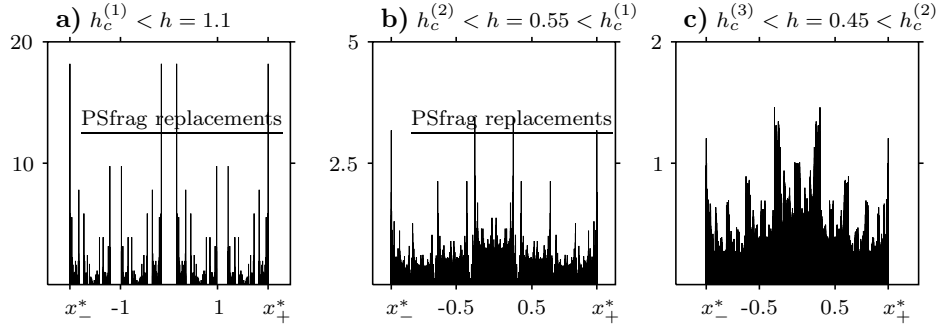


Figure 2: Qualitative changes of the behaviour of the invariant density $p(x)$.
 (a) the support of the measure is non-connected, (b) the support is connected but deep cuts in the measure density are visible (c) the support is connected and the deep cuts have vanished. ($\beta = 1$, $J = 1$ for all graphs.)

parameter h and for certain points x the sum even has only one term and the behaviour of the measure around such points can easily be analysed.

The map (3) generates a multifractal measure [5]. A quantity to characterize this type of measures is the so-called D_q -spectrum [14]. To obtain this quantity, the invariant interval $I = [x_-^*, x_+^*]$ is divided into $N(\epsilon)$ boxes of size ϵ and the partition function $Z_\epsilon(q) := \sum_{i=1}^{N(\epsilon)} P(i)^q$ is calculated. $P(i)$ is the measure of the box i and only boxes of non-vanishing measure $P(i)$ are taken into account. The partition function is found to scale as

$$Z_\epsilon(q) \sim k\epsilon^{(q-1)D_q}, \quad (10)$$

which defines the generalized fractal dimension D_q in the limit $\epsilon \rightarrow 0$. Here and in the following the symbol \sim always denotes the relation of asymptotic equality, i.e. $a(\epsilon) \sim b(\epsilon) \Leftrightarrow \lim_{\epsilon \rightarrow 0} a(\epsilon)/b(\epsilon) = 1$, or similar for sequences $(a_n)_{n \in \mathbb{N}}$ and $\lim_{n \rightarrow \infty}$. For $q > 0$ boxes with a high concentration of the measure contribute most to the generalized fractal dimension D_q whereas for negative q the most rarefied parts of the measure dominate.

In this article we investigate the dependence of the measure and its D_q -spectrum on the strength of the random field h , the inverse temperature β , and the coupling strength J . Given β and J there are several typical transitions of the invariant measure depending on the value of h .

For large h the support of the measure is non-connected and similar to a multi-scale Cantor set [5]. The first bands I_+ and I_- are well separated by a gap. Through iteration this gap has multiple images of decreasing width. The bands carrying the measure shrink to a set of Lebesgue measure zero as is typical for the Cantor construction.

At a critical value $h_c^{(1)}$ of h the support of the measure becomes connected for all $h \leq h_c^{(1)}$. The value of $h_c^{(1)}$ is determined by the overlap condition for

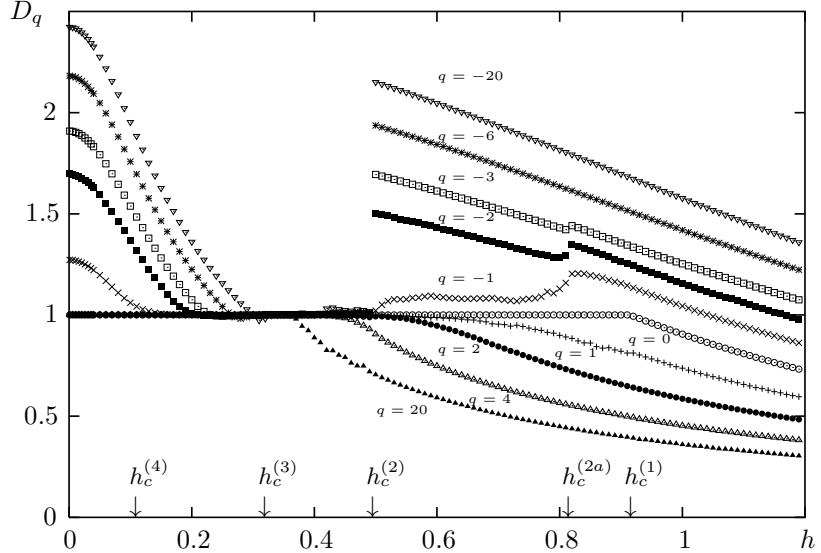


Figure 3: Generalized fractal dimensions D_q with $q = -20, -6, -3, -2, -1, 0, 1, 2, 4, 20$ versus the strength of the local magnetic random field h for the one-dimensional random field Ising model with coupling constant $J = 1$ and inverse temperature $\beta = 1$. The results shown were obtained by the thermodynamic formalism with the new natural partition developed by Behn and Lange [12]. The significance of the critical values $h_c^{(n)}$, $n = 1, \dots, 4$, and $h_c^{(2a)}$ is explained in the text.

the first bands, $f_-(x_+^*) = f_+(x_-^*)$. This results in [12]

$$h_c^{(1)} = \frac{1}{2\beta} \operatorname{arccosh}((e^{2\beta J} - 1)/2). \quad (11)$$

The transition can be seen in numerical approximations of the invariant measure density. An example is shown in Figure 2a and 2b. In the D_q -spectrum the transition is only visible as the point where D_0 becomes 1 (cf. Figure 3).

The most drastic change in the D_q -spectrum is observed at a critical value $h_c^{(2)} < h_c^{(1)}$. At this value of h the D_q -spectrum exhibits a massive drop of all generalized fractal dimensions D_q with $q < 0$ (cf. Figure 3). In the approximated invariant measure density deep cuts present for $h > h_c^{(2)}$ suddenly disappear at the critical value $h_c^{(2)}$ (cf. Figure 2b and 2c). The same remarkable behaviour of the D_q -spectrum has previously been found [15] in a model of learning in neural networks [16] and seems to be a very general feature of stochastic iterated function systems with bimodal probability distributions. The main objective of this article is the explanation of this type of transition and the application to

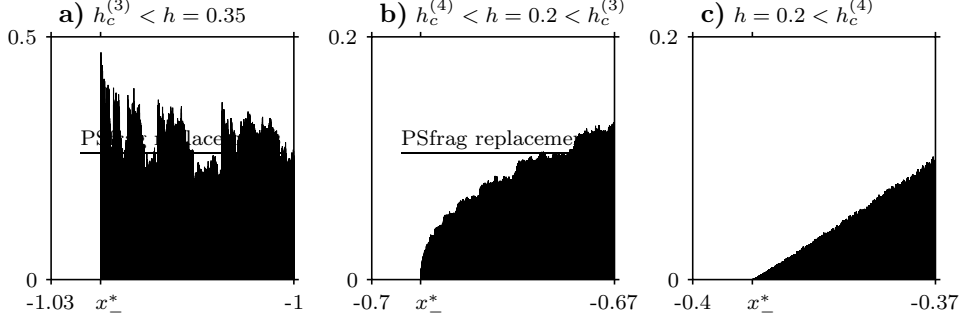


Figure 4: Qualitative changes of the behaviour of the invariant density $p(x)$ at the boundaries of the support. (a) $p(x_\pm^*) = \infty$, (b) $p(x_\pm^*) = 0$ but the slope of the coarse-grained measure density $\tilde{p}'(x_\pm^*)$ is infinite [15], (c) $p(x_\pm^*) = 0$ and $\tilde{p}'(x_\pm^*) = 0$. ($\beta = 1$, $J = 1$ for all graphs.)

the phase diagram of the multifractal measure associated with the random field Ising model in the multifractal thermodynamic formalism.

One can see another smaller drop in some of the generalized fractal dimensions D_q with $q < 0$ at a critical value $h_c^{(2a)} > h_c^{(2)}$. This drop is due to a similar mechanism as the larger one at $h_c^{(2)}$ as we will show below. Numerical studies suggest some more drops in the negative parts of the D_q -spectrum at critical values $h_c^{(2)} < h_c < h_c^{(2a)}$. These are probably also caused by this type of mechanism.

Finally there are two more transitions of the invariant measure which already have been studied before [12].

At $h_c^{(3)} \leq h_c^{(1)}$ the invariant measure density jumps from ∞ to 0 at the boundary x_+^* and x_-^* of I . This is easily understood by taking into account that only the leftmost (rightmost) band contributes to the measure density at x_-^* (x_+^*). Thus the measure density in the n -th approximation is given by

$$p_n(x_\sigma^*) = \frac{1}{2^n (f'_\sigma(x_\sigma^*))^n} p_0(x_\sigma^*). \quad (12)$$

Therefore $p_n(x_\sigma^*)$ diverges for $f'_\sigma(x_\sigma^*) < \frac{1}{2}$ and converges to 0 for $f'_\sigma(x_\sigma^*) > \frac{1}{2}$. The critical value $h_c^{(3)}$ is given by the condition $f'_\sigma(x_\sigma^*) = \frac{1}{2}$ and this yields [12]

$$h_c^{(3)} = \frac{1}{\beta} \operatorname{arcsinh} \left(2^{-\frac{3}{2}} (9e^{-4\beta J} + e^{4\beta J} - 10)^{\frac{1}{2}} (e^{4\beta J} - 1)^{-\frac{1}{2}} \right). \quad (13)$$

We only get one critical value because the restriction $h_+ = -h_- = h$ makes the two conditions for $\sigma = +$ and $\sigma = -$ equivalent. The transition is shown in Figure 4a and 4b. It is visible in the D_q -spectrum as the value of h where $D_{-\infty}$ begins to grow again for decreasing h (cf. Figure 3). As was shown in [15], the

generalized fractal dimension $D_{-\infty}$ has the value $D_{-\infty} = 1$ at this point and $D_{-\infty} > 1$ for $h < h_c^{(3)}$.

The last transition occurs at $h_c^{(4)} \leq h_c^{(3)}$ when the slope of the coarse grained invariant measure density at x_{\pm}^* jumps from $\mp\infty$ to 0. The slope can be deducted from the iterative approximation of the invariant measure density and this leads to the condition $f'_\sigma(x_\sigma^*) = \frac{1}{\sqrt{2}}$. This results in [12]

$$h_c^{(4)} = \frac{1}{\beta} \operatorname{arcsinh} \left(3 \cdot 2^{-\frac{5}{2}} - \frac{1}{2} - (3 \cdot 2^{-\frac{5}{2}} + \frac{1}{2}) e^{-4\beta J} \right)^{\frac{1}{2}}. \quad (14)$$

The transition is illustrated in Figure 4b and 4c with an approximation of the invariant measure density but is also not visible in the D_q -spectrum (cf. Figure 3). Again, $D_{-\infty}$ can be calculated analytically and takes the value $D_{-\infty} = 2$, see [15]. In fact, $D_{-\infty}$ can be calculated analytically for all $h < h_c^{(3)}$.

In the next section we give a detailed explanation of the mechanism causing the transitions at $h_c^{(2)}$ and $h_c^{(2a)}$ and discuss the resulting phase diagram of the invariant measure in the multifractal thermodynamic formalism. The key to the analysis of these transitions is that in the case of non-overlapping bands the correspondence between symbolic sequences $\{\sigma\}$ and the the fixed points $x_{\{\sigma\}}^*$ is one to one, i.e. we have a bijection between the set of inifinite symbolic sequences of + and - and the support of the invariant measure. In the case of overlapping bands this is not true for all these x but still for some. All x with unique periodic $\{\sigma\}$ sequence allow an analysis similar to the one previously applied to x_+^* and x_-^* [17, 18].

2 Orbits and their Contribution to the Invariant Measure

We group the points of the support of the invariant measure P_∞ into *orbits*. The orbit to a given symbolic sequence $\{\sigma\}$ consists of all preimages $f_{\{\sigma\}_n}^{-1}(x_{\{\sigma\}}^*)$ where $\{\sigma\}_n$ is the head of the first n symbols of $\{\sigma\}$.

In the case of a periodic sequence $\{\sigma\}$ with period length n the orbit therefore consists of the fixed points of the n functions $f_{\pi\{\sigma\}_n}$ in which $\{\sigma\}_n$ is the given finite aperiodic sequence defining the infinite periodic sequence and π denotes a cyclic permutation.

2.1 Singularity of Periodic Orbits

For the case of the fixed points (period one orbits) x_{\pm}^* of f_{\pm} it has been shown before that their singularity can be calculated explicitly [17, 18]. We generalize this concept to periodic orbits of arbitrary length.

In the following it is useful to consider the integrated measure P_∞ rather than the measure density p_∞ . As P_∞ is finite and continous we easily can work with the actual invariant measure instead of finite approximations P_n . The advantage will become more clear as we proceed.

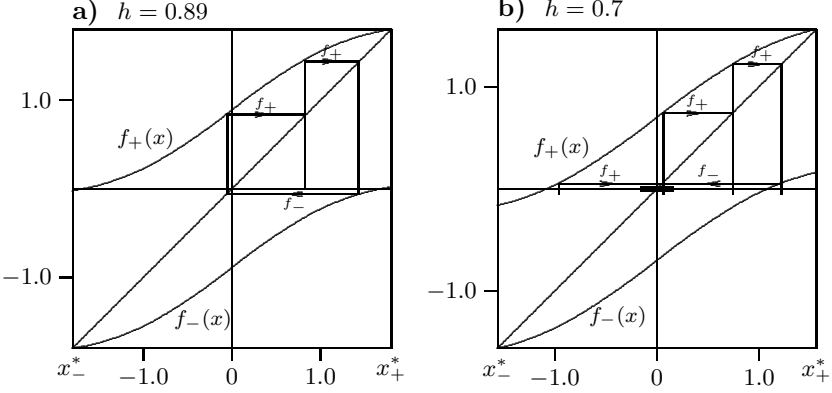


Figure 5: Orbits of period three for different values of h . (a) shows the case where no point of the orbit falls into the overlap region whereas in (b) the point $x_{\{-++\}}^*$ lies in the overlap region and has therefore two predecessors. ($\beta = 1$, $J = 1$ for all graphs.)

Let $y_i := f_{\sigma_i} \circ f_{\sigma_{i-1}} \circ \cdots \circ f_{\sigma_1}(x_{\{\sigma\}_n}^*)$ be the points of the periodic orbit defined by $\{\sigma\}_n$. We then have $y_n = y_0 = x_{\{\sigma\}_n}^*$ because of the fact that $x_{\{\sigma\}_n}^*$ is the fixed point of $f_{\{\sigma\}_n}$ by definition. An example for the periodic orbit of length 3 is shown in Figure 5.

In the case of non-overlapping bands the predecessor of each y_i with respect to the iteration of the Frobenius-Perron equation is uniquely determined to be y_{i-1} . There is only one term in the Frobenius-Perron equation at all y_i . We assume that the scaling limit

$$\lim_{\epsilon \rightarrow 0} \frac{P_\infty(x_{\{\sigma\}_n}^* + \frac{\epsilon}{2}) - P_\infty(x_{\{\sigma\}_n}^* - \frac{\epsilon}{2})}{\epsilon^{\alpha_{\{\sigma\}_n} + 1}} =: k \quad (15)$$

exists for some finite $k \neq 0$ and some $\alpha_{\{\sigma\}_n} \in \mathbb{R}$. As is shown in Appendix A this also implies

$$\lim_{\epsilon \rightarrow 0} \frac{P_\infty(f_{\{\sigma\}_n}^{-1}(x_{\{\sigma\}_n}^* + \frac{\epsilon}{2})) - P_\infty(f_{\{\sigma\}_n}^{-1}(x_{\{\sigma\}_n}^* - \frac{\epsilon}{2}))}{((f^{-1})'(x^*)\epsilon)^{\alpha_{\{\sigma\}_n} + 1}} = k. \quad (16)$$

The n -fold Frobenius-Perron equation yields

$$\begin{aligned} & P_\infty(x_{\{\sigma\}_n}^* + \frac{\epsilon}{2}) - P_\infty(x_{\{\sigma\}_n}^* - \frac{\epsilon}{2}) \\ &= \frac{1}{2^n} \left(P_\infty(f_{\{\sigma\}_n}^{-1}(x_{\{\sigma\}_n}^* + \frac{\epsilon}{2})) - P_\infty(f_{\{\sigma\}_n}^{-1}(x_{\{\sigma\}_n}^* - \frac{\epsilon}{2})) \right). \end{aligned} \quad (17)$$

We denote the expression on the left hand side as X and the one on the right hand side as $Y/2^n$ and thus have $X/Y = 1/2^n$. Inserting $1 = k/k$ and using the

above expressions for k with the introduced notation X and Y we get

$$\lim_{\epsilon \rightarrow 0} \left(\frac{X}{Y} \cdot \frac{Y / ((f_{\{\sigma\}_n}^{-1})'(x_{\{\sigma\}_n}^*) \epsilon)^{\alpha_{\{\sigma\}_n} + 1}}{X / \epsilon^{\alpha_{\{\sigma\}_n} + 1}} \right) = \frac{1}{2^n} \quad (18)$$

Most terms immediately cancel and we get

$$\frac{1}{((f_{\{\sigma\}_n}^{-1})'(x_{\{\sigma\}_n}^*))^{\alpha_{\{\sigma\}_n} + 1}} = \frac{1}{2^n}. \quad (19)$$

Therefore

$$\alpha_{\{\sigma\}_n} + 1 = \frac{n \ln 2}{\ln ((f_{\{\sigma\}_n}^{-1})'(x_{\{\sigma\}_n}^*))} \quad (20)$$

and with $(f_{\{\sigma\}_n}^{-1})'(x_{\{\sigma\}_n}^*) = (f'_{\{\sigma\}_n}(f_{\{\sigma\}_n}^{-1}(x_{\{\sigma\}_n}^*)))^{-1} = (f'_{\{\sigma\}_n}(x_{\{\sigma\}_n}^*))^{-1}$ we finally get

$$\alpha_{\{\sigma\}_n} = -1 - \frac{n \ln 2}{\ln (f'_{\{\sigma\}_n}(x_{\{\sigma\}_n}^*)}). \quad (21)$$

This equation is invariant under cyclic permutation of $\{\sigma\}_n$ such that the scaling behaviour of the invariant measure at all y_i , $i = 1, \dots, n$, is given by the same Hölder exponent $\alpha_{\{\sigma\}_n}$. If $\alpha_{\{\sigma\}_n} < 0$ the measure has a positive or strong singularity at all y_i and if $\alpha_{\{\sigma\}_n} > 0$ the singularity is negative or weak.

As $f'_{\{\sigma\}_n}(x_{\{\sigma\}_n}^*) = \prod_{i=1}^n f'_{\sigma_i}(y_{i-1})$, the derivatives $f'_{\sigma_i}(y_{i-1}) = A'(y_{i-1})$ at the points y_{i-1} of the periodic orbit determine the singularity $\alpha_{\{\sigma\}_n}$ and we finally have

$$\alpha_{\{\sigma\}_n} = -1 - \frac{n \ln 2}{\sum_{i=1}^n \ln A'(y_i)}. \quad (22)$$

Provided the sum $\frac{1}{n} \sum_{i=1}^n \ln A(y_i)$ converges as $n \rightarrow \infty$ for a given non-periodic orbit $\{\sigma\}$ we conjecture that the generalization of (22) to the non-periodic orbit $\{\sigma\}$ is possible. On the other hand the ergodicity of the invariant measure [13] implies that the singularity $\alpha(x)$ of P -almost all x is $D_1 - 1$ [20] such that for generic non-periodic orbits the singularity is already known. (It is a simple exercise to check on a computer that using the first 10^5 digits of the dual representation of π or e as a symbolic sequence, the value of α obtained from expression (22) is exactly the value $D_1 - 1$ shown in figure 3. This holds for all $h > h_c^{(1)}$ and of course the use of a random number generator instead of e or π yields the same result.)

When the bands begin to overlap with decreasing h for $h < h_c^{(1)}$, all $x \in [f_+(x_-^*), f_-(x_+^*)]$ have two predecessors under the iteration with f_+ and f_- and the Frobenius-Perron equation (5) has therefore two terms at these x . This changes the scaling behaviour at x compared to the case of only one predecessor.

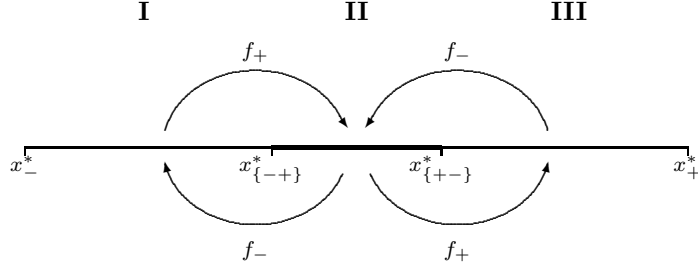


Figure 6: Mapping of the interval $I = [x_-^*, x_+^*]$ elucidating the importance of the interval $\mathbf{II} = [x_{-+}^*, x_{+-}^*]$. \mathbf{II} is mapped onto parts of **I** and **III** under f_- (f_+) which are itself preimages of **II** (all in the case of moderate overlap).

The scaling behaviour of all x belonging to orbits which do not touch the overlap interval is however not changed at all and the above considerations remain valid for these specific orbits.

If the parameter h is tuned the extent of the overlap region is changed as well as the location of the orbits. If (at least) one point x of a periodic orbit is in the overlap region there will be two terms in the Frobenius-Perron equation at this x . The two terms contribute singularities α and α' . Let us assume that α is the singularity contributed by the term in the Frobenius-Perron equation which is also present for larger h when the orbit does not touch the overlap region. If $\alpha' > \alpha$ nothing is changed by the second term and the singularity stays α . If $\alpha' < \alpha$, i.e. if the new singularity is stronger, the whole periodic orbit gets the new, stronger singularity α' . In the case $\alpha < 0$ this does not affect the D_q -spectrum very much. In the case $\alpha > 0$ though, a weak singularity is suddenly replaced by a stronger singularity. The new singularity α' at the point of first overlap, $h_c^{(2)}$, in fact is always rather strong as it stems from x_{\pm} where f'_{σ} is small. The replacement therefore may have a major impact on the D_q -spectrum.

The change in the singularity also happens for x in the support of the invariant measure which do not belong to periodic orbits but it is more subtle in this case as one preimage of x which may fall into the overlap region at some h in general only contributes once to the singularity at x and thus the change in the singularity at x is small. The disappearance of weak singularities in favour of strong singularities happens rather smoothly for these x .

2.2 Transition of the measure at $h_c^{(2)}$

As h is decreased the number of strong singularities increases at the expense of the number of weak singularities by the mechanism described above.

Special roles are played by the period one orbits $\{+\}$ and $\{-\}$ because they are never reached by the overlap and the period two orbit $\{+-\}$. Since x_{+-}^* is mapped to x_{-+}^* and vice versa and because f_{σ} is monotone, all points to the

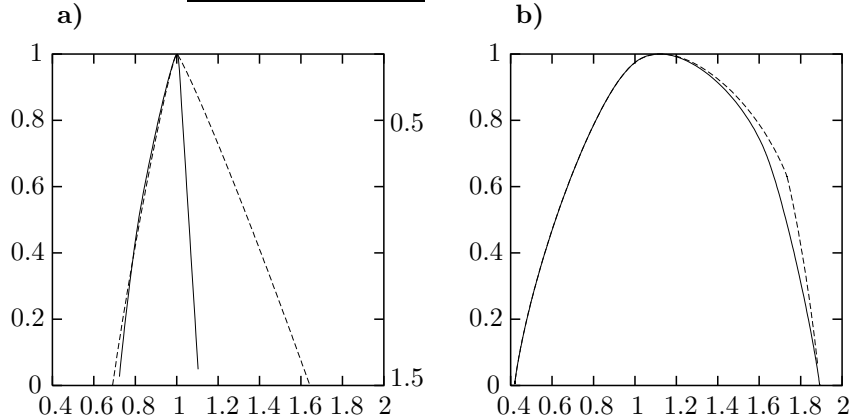


Figure 7: $f(\alpha)$ - spectrum of the invariant measure at different values of the noise strength h for $\beta = J = 1$. In a) the spectra at $h = 0.49385 > h_c^{(2)}$ (dashed line) and $h = 0.4938 < h_c^{(2)}$ (solid line) are shown. In b) the spectra are at $h = 0.8136 > h_c^{(2a)}$ (dashed line) and $h = 0.8128 < h_c^{(2a)}$ (solid line). The spectra were obtained by a numerical Legendre transform of the corresponding D_q - spectra. These were generated with the same algorithm as in figure 3 with a recursion depth of 21.

right of $x_{\{+-\}}^*$ are mapped to the right of $x_{\{-+\}}^*$ and all points to left of $x_{\{-+\}}^*$ are mapped to points left of $x_{\{+-\}}^*$. In the case of moderate overlap we therefore have the situation illustrated in Figure 6. We conclude that any periodic orbit of length greater than two must have at least one point inside $[x_{\{-+\}}^*, x_{\{+-\}}^*]$. Thus the $\{+-\}$ orbit is the last periodic orbit to be reached by the overlap region. The $\{+-\}$ orbit carries a very weak singularity as it always stays in regions with comparably large f'_σ and this causes a weak singularity in equation (22). For β and J in the vicinity of $\beta = J = 1$ one even can show that the orbit $\{+-\}$ carries the weakest singularity of all periodic orbits [19]. Because of its weak singularity and the fact that all other periodic orbits are reached by the overlap before $x_{\{+-\}}^*$ is reached, the $\{+-\}$ orbit practically solely determines all D_q with $q < 0$ if h is such that the overlap has nearly reached $x_{\{+-\}}^*$. When the overlap reaches $x_{\{+-\}}^*$, i.e. when $f_-(x_+^*) = x_{\{+-\}}^*$, the weak singularity of the $\{+-\}$ orbit is destroyed by the strong singularities contributed by $f_-(x_+^*)$ and $f_+(x_-^*)$ and all D_q with negative q collapse to $D_q = 1$. The critical value $h_c^{(2)}$ is therefore given by the condition $f_-(x_+^*) = x_{\{+-\}}^*$.

So far we have only discussed periodic orbits. Non-periodic orbits do not play a major role because they generically have the rather strong singularity $\alpha = D_1 - 1$ and also generically have points inside $[x_{-+}^*, x_{+-}^*]$ such that they are reached by the overlap before the $\{+-\}$ orbit is.

After the collapse the right part of the $f(\alpha)$ -spectrum of the invariant mea-

sure has vanished since the negative singularities have all been superseded by stronger ones (cf. Figure 7a). This behaviour has previously been observed in the case of the superposition of equal-scale [21] and multi-scale [22, 23] Cantor sets.

Let us now determine $h_c^{(2)}$ explicitly. In a first step we need explicit expressions for $x_+^* = -x_-^*$ and $x_{\{+-\}}^* = -x_{\{-+\}}^*$. The fixed point x_+^* is defined by $f_+(x_+^*) = x_+^*$. With the notation $z = e^{2\beta x_+^*}$ this yields the equation

$$z^2 - (e^{2\beta J}(e^{2\beta h} - 1))z - e^{2\beta h} = 0 \quad (23)$$

with the solution

$$x_+^* = \frac{1}{2\beta} \ln(K + \sqrt{K^2 + e^{2\beta h}}) \quad (24)$$

where $K = e^{2\beta J}(e^{2\beta h} - 1)/2$. The point $x_{\{-+\}}^*$ is defined by $f_-(f_+(x_{\{-+\}}^*)) = x_{\{-+\}}^*$. This is equivalent to $f_-(x_{\{+-\}}^*) = -x_{\{+-\}}^*$ or $A(x_{\{+-\}}^*) - h + x_{\{+-\}}^* = 0$. With $z = e^{2\beta x_{\{+-\}}^*}$ this yields

$$z^2 + e^{-2\beta J}(e^{2\beta h} - 1)z - e^{2\beta h} = 0 \quad (25)$$

and therefore

$$x_{\{+-\}}^* = \frac{1}{2\beta} \ln(\tilde{K} + \sqrt{\tilde{K}^2 + e^{2\beta h}}) \quad (26)$$

with $\tilde{K} = e^{-2\beta J}(e^{2\beta h} - 1)/2$.

The equation $f_-(x_+^*) = x_{\{+-\}}^*$ is equivalent to $x_+^* = x_{\{+-\}}^* + 2h$. With the explicit expressions for x_+^* and $x_{\{+-\}}^*$ we can write down this equation and after simplifying with Mathematica we get

$$z^2(z-1)^2[k^2(1+3z+3z^2+4z^3+3z^4+3z^5+z^6) - z^3 - k^4z^3] = 0, \quad (27)$$

in which $k = e^{2\beta J}$ and $z = e^{2\beta h_c^{(2)}}$. We denote the polynomial in the brackets as $P_6(z)$. Numerical evaluation shows that $P_6(z)$ has only one real root > 1 corresponding to a real solution $h_c^{(2)} \geq 0$. The resulting phase diagram for the transition at $h_c^{(2)}$ is shown in Figure 8. One clearly sees that there is a critical line $\beta(J)$ such that there is no phase transition possible for all $\beta < \beta(J)$. This line is given by the condition $h_c^{(2)} = 0$ corresponding to $z = 1$ in $P_6(z)$ which leads to

$$k^2(1+3+3+4+3+3+1) - 1 - k^4 = 0. \quad (28)$$

As $k = e^{2\beta J}$ this immediately gives

$$\beta(J) = \frac{1}{4J} \ln(9 + \sqrt{80}). \quad (29)$$

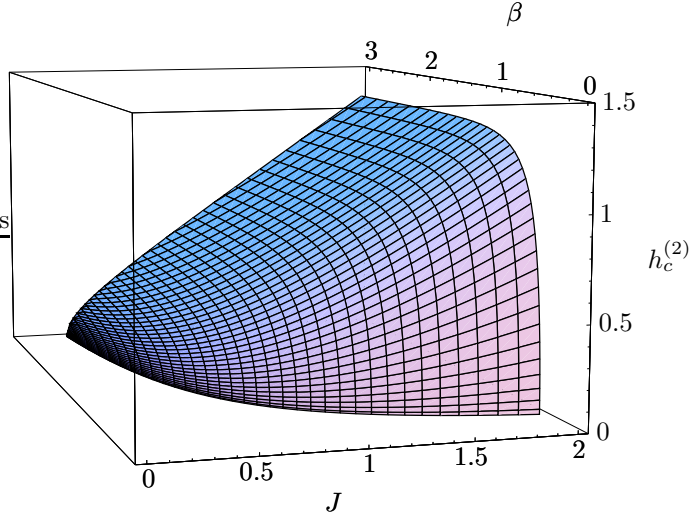


Figure 8: Surface plot of the critical value $h_c^{(2)}$ against β and J . The plot was obtained by numerical evaluation of the roots of the polynomial $P_6(z)$ as explained in the text.

2.3 Transition of the measure at $h_c^{(2a)}$

The smaller drop in parts of the negative D_q -spectrum is due to a similar mechanism as the one discussed in the last subsection. We consider the orbits of the form $\{-+(+)_n\}$ with $n \in \mathbb{N}$. Let $z_n := x_{\{-+(+)_n\}}^*$. We now prove that the sequence $(z_n)_{n \in \mathbb{N}}$ is a monotonously falling sequence with $\lim_{n \rightarrow \infty} z_n = f_{-+}(x_{\{+-\}}^*)$.

All orbits of the probabilistic iterated function system (IFS) given by f_+ and f_- are attractive because the IFS is hyperbolic. We therefore can approximate each $x_{\{\sigma\}_n}^*$ by the k -fold iteration $f_{\{\sigma\}_{n,k}}(x_0)$ of $f_{\{\sigma\}_n}$ applied to an arbitrary x_0 , i.e. $\lim_{k \rightarrow \infty} f_{\{\sigma\}_{n,k}}(x_0) = x_{\{\sigma\}_n}^*$ for any $x_0 \in I$. Now we consider two elements z_n and z_m with $m < n$. Let x_0 be some arbitrary point in I to the right of $x_{\{+-\}}^*$. After m -fold application of $f_{\{+-\}}$ to x_0 we apply $f_{\{+-\}}$ to get the first approximation of z_m and some more $f_{\{+-\}}$ followed by $f_{\{+-\}}$ to get the first approximation of z_n . As $f_{\{+-\}}$ is contractive each application of it puts x closer to the value $x_{\{+-\}}^*$ and thus $(f_{\{+-\}_n})(x_0) \leq (f_{\{+-\}_m})(x_0)$ which implies that the first approximation of z_n is smaller than the first approximation of z_m as $f_{\{+-\}}$ is monotonous. Further application of $f_{\{-+(+)_n\}}$ and $f_{\{-+(+)_m\}}$ respectively only enlarge the effect. Thus $z_n \leq z_m$ for $m < n$. Furthermore the orbit $\{+-\}$ as all other orbits is attractive. This implies $\lim_{n \rightarrow \infty} f_{\{+-\}_n}(x_0) = x_{\{+-\}}^*$ for any $x_0 \in I$. Let $\epsilon > 0$ and $x_0 \in I$, $x_0 > x_{\{+-\}}^* + \epsilon$ be arbitrary. Then $n \in \mathbb{N}$ exists with $f_{\{+-\}_n}(x_0) - x_{\{+-\}}^* < \epsilon$. This implies $f_{\{-+(+)_n\}}(x_0) -$

$f_{\{-+\}}(x_{\{+-\}}^*) < \epsilon$ and as the approximation numbers $f_{\{-+(+-)_n\}_k}$ fall with k also $z_n - f_{\{-+\}}(x_{\{+-\}}^*) < \epsilon$. This proves $\lim_{n \rightarrow \infty} z_n = f_{\{-+\}}(x_{\{+-\}}^*)$.

The orbit $\{-+(+-)_n\}$ has a weaker singularity than $\{-+(+-)_m\}$ for $m < n$ because it has more points in the vicinity of $x_{\{+-\}}^*$ and $x_{\{+-\}}^*$ where f'_σ is rather large and we therefore get a larger Hölder exponent α in (22).

The points z_n of the orbits $\{-+(+-)_n\}$ are the closest to the origin of all points of these orbits. This means that the orbit $\{-+(+-)_n\}$ is affected by the overlap iff $f_+(x_-^*) \leq z_n$. Furthermore the orbits carrying the stronger singularities get into the overlap region earlier than the ones with weaker singularities. The value of h for which $f_+(x_-^*) = f_{\{-+\}}(x_{\{+-\}}^*)$ is the first one with all $\{-+(+-)_n\}$ -orbits in the overlap. As the weaker singularities of the remaining orbits outside the overlap dominate the negative D_q spectrum for values of h close to $h_c^{(2a)}$ defined by the condition above, at least parts of the negative D_q -spectrum show a visible collapse at $h_c^{(2a)}$.

The above explanation of the transition of the invariant measure at $h_c^{(2a)}$ can be formulated from a slightly different point of view in terms of infinite sequences $\{\sigma\}$ and the corresponding possibly non-periodic orbits. The point $f_{\{-+\}}(x_{\{x-\}}^*)$ belongs to the $\{-+(+-)_\infty\}$ orbit. This orbit plays exactly the same role as the $\{+-\}$ orbit plays for the transition at $h_c^{(2)}$ above. It can be shown that all points of a non-periodic orbit carry the same singularity as in the case of periodic orbits. Even though in general we can not calculate the singularity of a non-periodic orbit the fact that the singularity of the $\{+-\}$ orbit and therefore of $x_{\{+-\}}^*$ is known allows us to calculate the singularity of the $\{-+(+-)_\infty\}$ orbit. Namely it is the same as the singularity of the $\{+-\}$ orbit. In the case that $\lim_{n \rightarrow \infty} \frac{1}{n} \sum_{i=1}^n \ln A'(y_i)$ exists this can intuitively be understood as the two extra terms $\ln A'(f_+(x_{\{+-\}}^*))$ and $\ln A'(f_-(f_+(x_{\{+-\}}^*)))$ cannot change the entire sum. We call orbits of this type, i.e. orbits of the form $\{\sigma\}_n(\{\tilde{\sigma}\}_m)_\infty$, non-periodic offshoots of the corresponding periodic orbit $\{\tilde{\sigma}\}_m$. In this language the $\{-+(+-)_\infty\}$ orbit is an offshoot of the $\{+-\}$ orbit. The offshoots of a periodic orbit always carry the same singularity as the periodic orbit itself.

It may be helpful to summarize the significance of the different parts of a symbolic sequence $\{\sigma\} = \{\sigma\}_n\{\tilde{\sigma}\}$ in the following way: The head $\{\sigma\}_n$ determines the position of the corresponding fixed point $x_{\{\sigma\}}^*$ and the tail $\{\tilde{\sigma}\}$ determines the singularity at this point.

For very small q the $\{+-\}$ -orbit and its offshoots of the form $\{(+)_n(-)_\infty\}$ and $\{(-)_n(+)_\infty\}$ with their weak singularity already dominate at $h_c^{(2a)}$ and thus the transition is not visible in D_q with $q \ll 0$.

Like at $h_c^{(2)}$, the transition is also visible in the $f(\alpha)$ -spectrum. For $h \rightarrow h_c^{(2a)} + 0$ a cusp develops and the spectrum collapses to a smooth form again at $h_c^{(2a)}$ (cf. Figure 7b).

The explanation of the smaller drop in parts of the negative D_q -spectrum exhibits a perfect match with numerical results. In Figure 9 this is illustrated

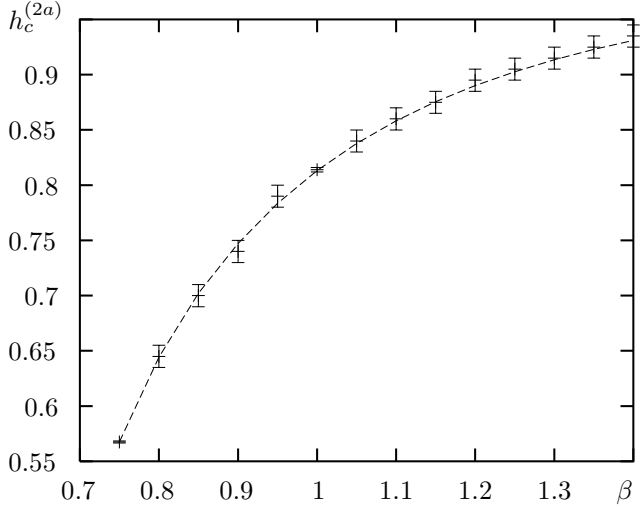


Figure 9: Comparison of the analytical expression for $h_c^{(2a)}$ (dashed line) to numerical results for the small drop in the D_q -spectrum (errorbars) at $J = 1$. The errors are estimated and mainly due to the imprecise determination of the exact location of the drop in the numerically approximated D_q -spectra.

for some values of β and $J = 1$.

3 Concluding Remarks

The formula given in the last two sections allow to draw a complete phase diagram for the phase transitions of the invariant probability measure of the auxiliary random field x we introduced in section 1. It should be emphasized at this point that these ‘phase transitions’ are not phase transitions of physical quantities like the (local) magnetisation or the Edwards-Anderson parameter. The phase diagram is shown in Figure 10.

The scenario explained in this article is also found in other applications of stochastic maps [15]. The essential features we used for the explanation of this mechanism are:

1. A stochastic map with two smooth monotonous functions $f_+(x) > f_-(x)$, depending on a control parameter h .
2. A non-chaotic dynamic, i.e. $f_{\pm}''(x) < 1$ almost everywhere, such that a finite invariant interval $I = [x_+^*, x_-^*]$ exists.
3. The scaling property (15) at $x_{\{\sigma\}_n}^*$ for most $\{\sigma\}_n$.
4. $f'_-(x_{\{+-\}}^*)$ and $f'_+(x_{\{-+\}}^*)$ are sufficiently large.

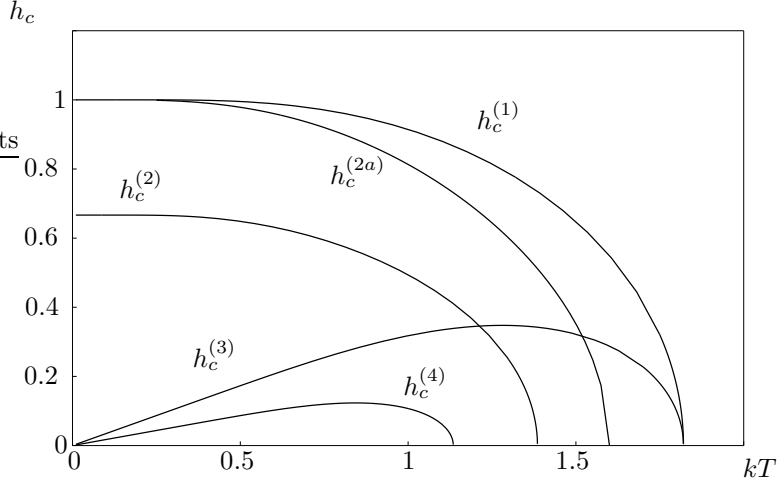


Figure 10: Phase diagram for the phase transitions of the invariant measure derived from the random field Ising model. The $h_c^{(n)}$ are as defined in the text. It is remarkable that the lines of $h_c^{(2)}$ and $h_c^{(3)}$ as well as the lines of $h_c^{(2a)}$ and $h_c^{(3)}$ intersect.

5. The dependence on the control parameter h is such that the conditions $f_-(x_+^*) = x_{\{+-\}}^*$ and $f_+(x_-^*) = f_{\{-+\}}(x_{\{+-\}}^*)$ can be fulfilled by tuning h .

We concede that some of the above explanations are not given with full mathematical rigour. Furthermore we have not addressed the question whether there is a similar behaviour for discrete stochastic mappings in higher dimensions or for discrete distributions of the noise with more than two possible values, which also seems to be very interesting. We are likewise interested in the exact functional dependence of the D_q -spectrum on h right at the transition points which has not been thoroughly investigated yet.

Acknowledgements

Two of us (H. P. and U. B.) acknowledge valuable discussions with Dr. Adrian Lange in a very early stage of this work.

A Connections between Scaling Relations

In this Appendix we show that the assumed scaling relation

$$\lim_{\epsilon \rightarrow 0} \frac{P_\infty(x_{\{\sigma\}_n}^* + \frac{\epsilon}{2}) - P_\infty(x_{\{\sigma\}_n}^* - \frac{\epsilon}{2})}{\epsilon^{\alpha_{\{\sigma\}_n}+1}} =: k \quad (30)$$

implies that the limit

$$\lim_{\epsilon \rightarrow 0} \frac{P_\infty(f_{\{\sigma\}_n}^{-1}(x_{\{\sigma\}_n}^* + \frac{\epsilon}{2})) - P(f_{\{\sigma\}_n}^{-1}(x_{\{\sigma\}_n}^* - \frac{\epsilon}{2}))}{((f_{\{\sigma\}_n}^{-1})'(x_{\{\sigma\}_n}^*) \epsilon)^{\alpha_{\{\sigma\}_n}+1}} \quad (31)$$

exists and is equal to k . In the following we drop the indices $\{\sigma\}_n$ to improve readability and denote the expression in (31) as $Q(\epsilon)$. Applying the mean value theorem to f^{-1} in $Q(\epsilon)$ and using $f^{-1}(x^*) = x^*$ yields

$$Q(\epsilon) = \frac{P_\infty(x^* + (f^{-1})'(x^* + \delta_1)\frac{\epsilon}{2}) - P_\infty(x^* - (f^{-1})'(x^* - \delta_2)\frac{\epsilon}{2})}{((f^{-1})'(x^*) \epsilon)^{\alpha+1}} \quad (32)$$

with some $\delta_1, \delta_2 \in [0, \frac{\epsilon}{2}]$. Now let $(f^{-1})'_{\min}$ be the minimum of $(f^{-1})'(x^* + \delta_1)$ and $(f^{-1})'(x^* - \delta_2)$. Because f^{-1} is strictly monotonously growing we have $(f^{-1})'_{\min} > 0$. Using the fact that P_∞ is monotonously growing as well we get the lower estimate

$$B(\epsilon) \geq \frac{P(x^* + (f^{-1})'_{\min}\frac{\epsilon}{2}) - P(x^* - (f^{-1})'_{\min}\frac{\epsilon}{2})}{((f^{-1})'(x^*) \epsilon)^{\alpha+1}} \quad (33)$$

$$= \frac{P(x^* + (f^{-1})'_{\min}\frac{\epsilon}{2}) - P_\infty(x^* - (f^{-1})'_{\min}\frac{\epsilon}{2})}{((f^{-1})'_{\min}\epsilon)^{\alpha+1}} \cdot \left(\frac{(f^{-1})'_{\min}\epsilon}{(f^{-1})'(x^*) \epsilon} \right)^{\alpha+1}. \quad (34)$$

The quotient of $(f^{-1})'_{\min}$ and $(f^{-1})'(x^*)$ converges to 1 and thus

$$\lim_{\epsilon \rightarrow 0} B(\epsilon) \geq \lim_{\epsilon \rightarrow 0} \frac{P(x^* + (f^{-1})'_{\min}\frac{\epsilon}{2}) - P(x^* - (f^{-1})'_{\min}\frac{\epsilon}{2})}{((f^{-1})'_{\min}\epsilon)^{\alpha+1}} = k. \quad (35)$$

Using the maximum of $(f^{-1})'(x^* + \delta_1)$ and $(f^{-1})'(x^* - \delta_2)$ instead of the minimum we get in the same fashion the upper estimate

$$\lim_{\epsilon \rightarrow \infty} Q(\epsilon) \leq k. \quad (36)$$

Both estimates together give the conjectured result $\lim_{\epsilon \rightarrow 0} Q(\epsilon) = k$.

References

- [1] Bruinsma R and Aeppli G 1983 *Phys. Rev. Lett.* **50** 1494
- [2] Györgyi G and Ruján P 1984 *J. Phys. C* **17** 4207
- [3] Szépfalusy P and Behn U 1987 *Z. Phys. B* **65** 337
- [4] Behn U and Zagrebnov V A 1987 *J. Stat. Phys.* **47** 939
- [5] Behn U and Zagrebnov V A 1988 *J. Phys. A : Math. Gen.* **21** 2151
- [6] Behn U and Zagrebnov V A 1988 *Phys. Rev. B* **38** 7115
- [7] Bene J and Szépfalusy P 1988 *Phys. Rev. A* **37** 1703
- [8] Bene J 1989 *Phys. Rev. A* **39** 2090
- [9] Tanaka T, Fujisaka H and Inoue M 1989 *Phys. Rev. A* **39** 3170
- [10] Tanaka T, Fujisaka H and Inoue M 1990 *Prog. Theor. Phys.* **84** 584
- [11] Behn U, Priezzhev V B and Zagrebnov V A 1990 *Physica A* **167** 481
- [12] Behn U and Lange A 1992 *From Phase Transitions to Chaos* ed Györgyi G, Kondor I, Sasvári L and Tél T (Singapore: World Scientific) 217
- [13] Behn U and Zagrebnov V A 1987 JINR, E 17-87-138 Dubna
- [14] Halsey T C, Jensen M H, Procaccia I and Shraiman B I 1989 *Phys. Rev. A* **33** 1141
- [15] Behn U, van Hemmen J L, Kühn R, Lange A, and Zagrebnov V A 1993 *Physica D* **68** 401
- [16] van Hemmen J L, Keller G and Kühn R 1988 *Europhys. Lett.* **5** 663
- [17] Behn U, van Hemmen J L, Kühn R, Lange A and Zagrebnov V A 1994 *On Three Levels* ed M Fannes et al (New York: Plenum Press) 399
- [18] Patzlaff H, Behn U and Lange A 1997 *FRACTAL FRONTIERS, Fractals in the Natural and Applied Sciences* ed M M Novak and T G Dewey (Singapore: World Scientific) 95
- [19] Patzlaff H 1998 *Dissertation* (Universität Leipzig)
- [20] Young L S 1982 *Ergodic Theory and Dyn. Systems* **2** 109
- [21] Radons G 1995 *Phys. Rev. Lett.* **75** 2518
- [22] Radons G and Stoop R 1996 *J. Stat. Phys.* **82** 1063
- [23] Stoop R and Steeb F-H 1997 *Phys. Rev. E* **55** 6589